A SENSORLESS MODEL PREDICTIVE CONTROL FRAMEWORK FOR WAVE ENERGY CONVERTERS UTILIZING EXTENDED KALMAN FILTER-BASED EXCITATION FORCE ESTIMATION

Tongzhou Liu[1], Lixun Zhu[1], Xinglong Jin[2], Zhixin Huang[1], Bo Li[3], Xin Jin[3]

[1] Shanghai Maritime University, Shanghai 201306, China
[2]Taiyuan Heavy Industry (Shanghai) Equipment Technology Co., Ltd, Shanghai, China
[3]Liaoning Inspection, Examination and Certification Centre, Shenyang 110031, China
202330210081@stu.shmtu.edu.cn

Keywords: WAVE ENERGY CONVERTER, EXTENDED KALMAN FILTER, MPC, LINEAR REGRESSION

Abstract

Wave energy converters (WECs) face significant challenges in control performance due to system nonlinearity, dynamic parameter coupling, and reliance on costly physical sensors. To address these issues, this paper proposes a sensorless control strategy that combines an Extended Kalman Filter (EKF)-based excitation force estimation with Model Predictive Control (MPC). The EKF estimates excitation forces in real time using measurable buoy motion states—namely, heave velocity and displacement—eliminating the need for direct wave force measurements. The estimated forces are then integrated into an MPC framework to address parameter coupling among hydrodynamics, power take-off (PTO) damping, and generator load. Simulation results demonstrate that the proposed method achieves comparable control accuracy to conventional MPC strategies based on known excitation inputs, while significantly reducing system complexity and sensor costs.

1 Introduction

Under the dual pressures of global climate crisis response and energy transition, renewable energy technologies have become the core driver for reshaping human energy systems. Wave power generation, as a renewable energy source, offers clean and sustainable characteristics that effectively reduce dependence on fossil fuels. Its development not only mitigates global climate change but also promotes optimization and transformation of energy structures [1]. Additionally, the widespread availability of wave energy resources in coastal regions provides new possibilities for local economic development and energy self-sufficiency. Wave Energy Converters (WECs) are recognized as effective tools for capturing ocean wave energy [2].

However, existing control strategies often exhibit inefficient energy conversion and system stability issues under irregular wave conditions. In recent years, numerous control strategies—such as impedance matching [3]and optimal velocity tracking [4]—have been proposed to optimize WEC energy conversion. Although these methods perform well in specific cases, they rely heavily on accurate modeling and degrade significantly under wide wave frequency variations. Thus, the adaptability and robustness of current approaches remain limited [5]. Model Predictive Control (MPC) has attracted growing attention due to its intuitive design principles, ability to handle multi-variable systems, and strong performance in managing nonlinear constraints.

One of the main problems in MPC applications is the accurate prediction of the wave excitation force, which is a key input in the dynamic modeling of WEC systems, and which is usually unpredictable and varies with the waves [6]. For example, in [7] a pressure sensor is used to measure the total wave force minus the radiative and viscous forces to obtain an approximate excitation force, while in [8] the wave excitation force is assumed to be a known quantity.

This paper proposes a linear regression Kalman filter-based method for predicting wave excitation forces, aimed at enhancing traditional model predictive control by replacing the need for real-time measurement and prediction of wave excitation forces during MPC operation., with the simple and easy-to-measure velocity information. Simulation results show that the performance of this method is very close to the traditional MPC control method based on known future excitation force information.

The mathematical model of the point absorbing wave energy converter is developed in Section II. The proposed control strategy is appropriately derived in Section III. The results of this study are presented in Section IV. Finally, some conclusions are drawn in Section V.

2. Methodology

2.1 Equation of motion

The focus of this study is a point-absorbing WEC, shown in Fig. 1. It includes three components: A buoyant structure positioned at the sea surface, an energy conversion mechanism (PTO), and a stationary base structure.

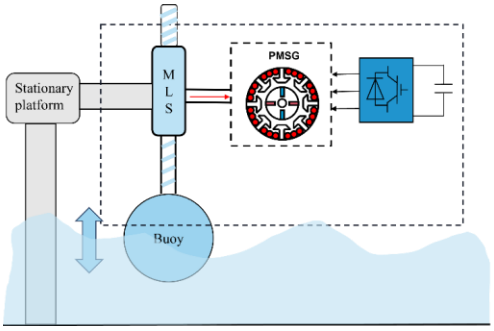

Fig. 1 Schematic diagram of a point absorber wave energy converter (WEC)

The WEC extracts energy from the relative heave motion of the floating body. The mathematical representation of the floating device's motion dynamics is expressed through the following relationship:

$$M\ddot{z}(t)=F_{exc}(t)+F_{pto}(t)-F_h(t)-F_{rad}(t) \tag{1}$$

Here, z represents the vertical displacement of the float near its equilibrium position, M denotes the float's mass, F_{pto} is the power take-off (PTO) force, and F_h, F_{rad} correspond to the hydrostatic and radiative forces, respectively, as shown in the equation below:

$$F_h(t)=K_h z(t) \tag{2}$$

$$F_{rad}(t)=m_\infty \ddot{z}(t)+\int_0^t h_r(t-\tau)\dot{z}(t)d\tau \tag{3}$$

where m_∞ refers to the extra mass at an infinite frequency, h_r is the radiative convolution term, and K_h is the fluid stiffness, expressing the convolution term in the radiative force in state space:

$$\begin{cases}\int_0^t k(t-\tau)\dot{x}(t)d\tau \approx C_r \underline{x}_r(t)\\ \underline{x}_r(t)=A_r\underline{x}_r(t)+B_r\dot{z}(t)\end{cases} \tag{4}$$

where A_r, B_r , C_r are the correlation matrices, which can be calculated by NEMOH [9], and $\underline{x}_r$ is the radiative subsystem state.

2.2 Model predictive control

By integrating equations (1) to (4), the dynamic model of the point absorber WEC can be derived as follows:

$$\begin{cases}(M+m_\infty(\omega))\ddot{x}(t)+C_r\underline{x}_r-K_s x(t)=u(t)+w(t)\\ \underline{x}_r(t)=A_r\underline{x}_r(t)+B_r\dot{z}(t)\end{cases} \tag{5}$$

The system can be represented using a linear time-invariant state-space model, which is formulated as:

$$\begin{cases}\dot{x}_c(t)=A_c x_c(t)+B_c u(t)+B_c w(t)\\ y_c(t)=C_c x_c(t)\end{cases} \tag{6}$$

Where: $x_c(t)=\begin{bmatrix}z(t) & \dot{z}(t) & \underline{x}_r(t)\end{bmatrix}^T$, $y_c(t)=\begin{bmatrix}z(t) & \dot{z}(t)\end{bmatrix}^T$, $u(t)=F_{\mathrm{PTO}}(t)$, $w(t)=F_{\mathrm{exc}}(t)$.

For the deployment of the model predictive control (MPC) strategy, the continuous-time state-space representation requires discretization. The resulting discrete-time formulation is mathematically defined as:

$$\begin{cases}\underline{x}(k+1)=A_d\underline{x}(k)+B_d u(k)+B_d w(k)\\ y(k)=C_d\underline{x}(k)\end{cases} \tag{7}$$

where: $A_d=e^{A_cT_s}$, $B_d=\int_0^{T_s}e^{A_cT_s}d\tau B_c$, $C_d=C_c$, T_s is the sampling time.

An incremental representation is used in the state vectors and the input increments are used as decision variables in the state space model, which in turn creates the MPC prediction model. The discrete state space expression using the incremental form is:

$$\begin{cases}x(k+1)=Ax(k)+B\Delta u(k)+B_w w(k)\\ y(k)=Cx(k)\end{cases} \tag{8}$$

The current input state $x(k)=\begin{bmatrix}x(k) & u(k-1)\end{bmatrix}^T$ and output states are $y(k)=\begin{bmatrix}y(k) & u(k-1)\end{bmatrix}^T$.

Where: $A=\begin{bmatrix}A_d & B_d\\ 0 & 1\end{bmatrix}$, $B=\begin{bmatrix}B_d\\ 1\end{bmatrix}$, $B=\begin{bmatrix}B_d\\ 0\end{bmatrix}$, $C=\begin{bmatrix}C_d & 0\\ 0 & 1\end{bmatrix}$.

At time step k, the prediction model forecasts system outputs over a prediction horizon of N steps:

$$\hat{Y}=\left[y(k+1),y(k+2),\cdots,y(k+N)\right]^T \tag{9}$$

Upcoming wave excitation force can be mathematically represented as:

$$\hat{W}=\left[\hat{W}_k,\hat{W}_{k+1},\cdots,\hat{W}_{k+N}\right]^T \tag{10}$$

The anticipated control signal variations within the prediction horizon are formulated as:

$$\Delta\hat{U}=\left[\Delta\hat{U}(k),\Delta\hat{U}(k+1),\cdots,\Delta\hat{U}(k+N)\right]^T \tag{11}$$

The formula for calculating $\hat{Y}$ is:

$$\hat{Y}=Gx(k)+H_d\Delta\hat{U}+H_w\hat{W} \tag{12}$$

2.3Estimation of excitation force

As outlined by equations (8) and (9), successful deployment of model predictive control (MPC) in wave energy conversion systems demands real-time access to hydrodynamic excitation force forecasts spanning the entire prediction horizon to ensure optimal control actions. Existing wave parameter acquisition methods usually rely on costly specialized instruments (e.g., contact wave height monitors or distributed pressure sensing arrays), which make it difficult to directly access the dynamic wave loads acting on the device. In addition, the need for real-time prediction of wave excitation forces further increases the system's hardware arithmetic burden in terms of dynamic modeling and real-time computation.

Additional control devices not only increase the installation costs of Wave Energy Converters (WECs), reducing their economic feasibility, but also introduce additional uncertainties, thereby compromising the reliability of WECs under real ocean conditions. In this context, it becomes essential to replace the excitation force with measurable physical quantities. Compared to excitation forces, position and velocity sensors offer greater cost-effectiveness, durability, and reliability, making them more suitable for large-scale applications. However, sensor data is often affected by noise and interference, which can impair the accuracy and stability of the system. To resolve this limitation, the schematic diagram in Fig. 2 illustrates the integration of: we introduce the Extended Kalman Filter (EKF) to denoise the raw sensor data and enhance the accuracy of the float's velocity and position measurements. EKF effectively removes random noise from the sensor data, providing more accurate dynamic information. Subsequently, a linear regression analysis is employed to establish the relationship between the float's velocity and the excitation force. This regression model is then used to replace the excitation force information required for Model Predictive Control (MPC) with the processed velocity data, thereby simplifying the system structure and enhancing its reliability.

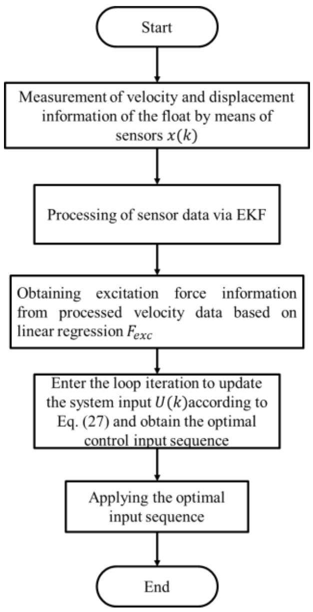

Fig. 2 Flowchart of MPC control for EKF-based excitation force estimation

The nonlinear system model for the floating body motion under EKF is defined as:

$$\begin{aligned} x_k &= f\left(x_{k-1}, u_{k-1}\right) + w_{k-1} \\ z_k &= h\left(x_k\right) + v_k \end{aligned} \tag{13}$$

where $f(\cdot)$ and $h(\cdot)$ denote the state and output (measurement) functions, respectively. The vectors x_{k-1}, u_{k-1}, and w_{k-1} represent the estimated state, input, and process noise at time k−1. The measurement function $h(\cdot)$ maps the estimated state vector x_k, and the measurement noise vector v_k, while z_k refers to the estimated output vector.

Once the EKF processes the velocity and displacement signals, these are used to reconstruct the empirical equations to determine the wave excitation force, along with the float's rise and sinking rates. Linear regression examines the relationship between two variables, x and y. It is commonly used to fit an empirical straight line to an ideal sample. Suppose that for each value of:

$$Y_i \sim N\left(\alpha + \beta x_i, \sigma^2\right) \tag{14}$$

Where α, β, σ^2 and are unknown parameters that do not depend on. Denoted as:

$$\varepsilon_i = Y_i - \left(\alpha + \beta x_i\right), \left(i = 1, 2, \cdots, n\right) \tag{15}$$

The parameters α and β are estimated using the least squares method, which allows the construction of the empirical regression equation for Y in relation to x.

2.4 Implementation methods

Based on the modeling of the response relationship between pendant velocity and wave excitation force, the floating body pendant velocity is set as a predictor variable, and a linear regression method is used to construct an empirical relationship model between the two. Within the MPC framework, a dataset of float heave velocities is collected from the point absorber system, and a linear mapping between velocity and excitation force is established as:

$$F_{exc}\left(t\right) = b + a\dot{z}\left(t\right) \tag{16}$$

where a and b are regression parameters fitted on the basis of measured data.

Combining formulas. (6)(16) yields a linear regression-based kinetic model of the point-absorbing wave energy converter, which is expressed as:

$$\begin{gathered} \left(M + m_\infty\right)\ddot{z}\left(t\right) + \int_0^t h_r\left(t - \tau\right)\dot{z}\left(t\right)d\tau + K_h z\left(t\right) = \\ u\left(t\right) + a\dot{z}\left(t\right) \end{gathered} \tag{17}$$

The updated linear time-invariant state-space model is give n by:

$$\begin{cases} \dot{x}_L\left(t\right) = A_{Lc}x_c\left(t\right) + B_c u\left(t\right) \\ y_L\left(t\right) = C_c x_c\left(t\right) \end{cases} \tag{18}$$

Where: $A_{Lc} = \begin{bmatrix} 0 & 1 & 0 \\ \dfrac{-K_h}{M + m_\infty} & \dfrac{a}{M + m_\infty} & \dfrac{-C_r}{M + m_\infty} \\ 0 & B_r & A_r \end{bmatrix}$,

$B_c = \begin{bmatrix} 0 \\ \dfrac{1}{M + m_\infty} \\ 0 \end{bmatrix}$, $C_c = \begin{bmatrix} 1 & 0 & 0 \\ 0 & 1 & 0 \end{bmatrix}$.

The updated discrete state-space equation is as follows:

$$\begin{cases} \underline{x}_L\left(k+1\right) = A_{Ld}\underline{x}\left(k\right) + B_d u\left(k\right) \\ y_L\left(k\right) = C_d\underline{x}\left(k\right) \end{cases} \tag{19}$$

Where: $A_{Ld} = e^{A_L T_s}$, $B_{Ld} = \int_0^{T_s} e^{A_{Lc}T_s} d\tau B_c$, $C_{Ld} = C_c$.

Under the MPC paradigm, the dynamical system formulation employs the control input variation $u(k)$ as the optimization parameter, governed by the discrete-time state transition equation:

$$\begin{cases} x_L\left(k+1\right) = A_L x_L\left(k\right) + B_L \Delta u_L\left(k\right) \\ y_L\left(k\right) = C_L x_L\left(k\right) \end{cases} \tag{20}$$

At each time step k, the prediction model projects system outputs over a future horizon of N steps:

$$\hat{Y}_L = \left[y_L(k+1), y_L(k+2), \cdots, y_L(k+N) \right]^T \tag{21}$$

Predict the incremental sequence of control quantities in the time domain:

$$\Delta\hat{U}_L = \left[\Delta\hat{U}_L(k), \Delta\hat{U}_L(k+1), \cdots, \Delta\hat{U}_L(k+N) \right]^T \tag{22}$$

The expression for computing $\hat{Y}$ is:

$$\hat{Y}_L = G_L x_L(k) + H_L \Delta\hat{U}_L \tag{23}$$

Where: $$G_L = \begin{bmatrix} G_L A_L \\ G_L A_L^2 \\ \vdots \\ G_L A_L^N \end{bmatrix}^T,$$

$$H_L = \begin{bmatrix} C_L B_L & 0 & \cdots & 0 \\ C_L A_L B_L & C_L B_L & \ddots & \vdots \\ \vdots & \ddots & \ddots & 0 \\ C_L A_L^{N-1} B_L & \cdots & C_L A_L B_L & C_L B_L \end{bmatrix}.$$

2.4 Optimization formulation

In the predictive control of a wave energy device (WEC), the peak energy that can be captured by the system in the time domain T corresponds to the mechanical energy output of the power take-off unit (PTO), which is quantified by the expression:

$$E_m = -(M + m_\infty) \int_t^{t+T} u(\tau)\dot{z}(\tau) d\tau \tag{24}$$

Thus, the objective function for discretization is defined as:

$$J(k) = \sum_{i=1}^{N} u(k+i-1)\dot{Z}(k+i) \tag{25}$$

The objective function is then transformed into a standard quadratic form, as shown:

$$J(k) = \frac{1}{2} \hat{Y}_L^T(k) Q \hat{Y}_L(k) \tag{26}$$

By substituting equation (17) into equation (20), the quadratic expression for J with respect to Δu is derived. Terms irrelevant to the decision variable Δu are eliminated, yielding the objective function as follows:

$$J(k) = \frac{1}{2} \Delta\hat{U}^T E \Delta\hat{U} + \Delta\hat{U}^T f, M\Delta\hat{U} \le b \tag{27}$$

$$E = H_L^T Q H_L \qquad f = H_L^T Q G_L x_L(k)$$

The Q is constructed using a chunked diagonal construction, with each submodule q_{k+i} arranged in N cycles on the main diagonal ($i \in [1, N]$), which is characterized in Ref. The system constraints are fully described by the linear inequality $M\Delta\hat{U} \le b$, where M characterizes the system parameter matrix and b defines the set of constraint boundaries.

$$M = \begin{bmatrix} I \\ -I \\ D \\ -D \end{bmatrix}, b = \begin{bmatrix} \Delta u_{\max} 1 \\ -\Delta u_{\max} 1 \\ (u_{\max} - u_{k-1})1 \\ -(u_{\max} + u_{k-1})1 \end{bmatrix}, Q = \begin{bmatrix} q_{k+1} & 0 & \cdots & 0 \\ 0 & q_{k+2} & \ddots & \vdots \\ \vdots & \ddots & \ddots & 0 \\ 0 & \cdots & 0 & q_{k+N_p} \end{bmatrix},$$

$$q_{k+i} = \begin{bmatrix} 0 & 0 & 0 \\ 0 & 0 & 1 \\ 0 & 1 & 0 \end{bmatrix}$$

The mathematical programming framework of the control system is solved by leveraging the quadratic programming solver "quadprog" in MATLAB. Following the receding horizon mechanism of model predictive control (MPC), solely the initial actuation command is implemented during individual control intervals, with successive optimization cycles executed iteratively across sequential sampling periods.

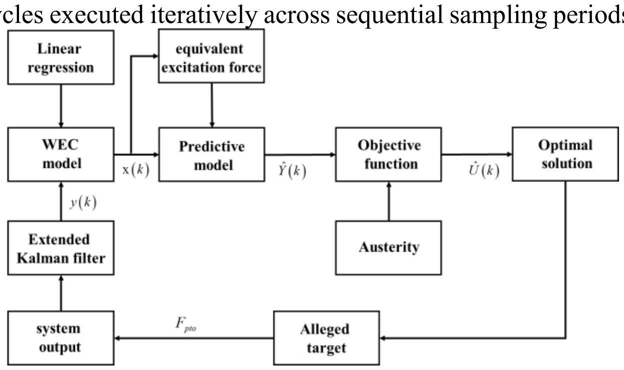

Fig. 3 Point Absorber WEC Control Block Diagram

3 Simulation Results

This study adopts a linear session-based predictive control framework to manage the operational dynamics of a cylindrical point-absorbing wave energy converter. The numerical validation demonstrates system performance under specified hydrodynamic conditions: a temporal resolution of 50ms ($\Delta\tau$= 0.05s), buoy geometric parameters (radius = 0.88 m, submergence depth = 0.53m, inertial mass = 858 kg), and stochastic wave excitation characterized by a JONSWAP [10] spectrum (significant wave height Hs=0.15 m, spectral peak period $T_p = 3.5\ s$) over a 200-second simulation horizon. Hydrodynamic parameters were computed via potential flow simulations using the open-source BEM solver NEMOH, with full system specifications detailed in the parametric compilation table.

Table 1. System parameters used in the simulation.

Notation	Description	Value
ρ	Sea-water density	1000 kg/m3
g	Gravitational acceleration	9.8 N/kg
M	Floater mass	858 kg
m_∞	Added mass	782 kg
K_h	Hydrostatic stiffness	23981 N/m
F_{pto}	Input limit	1200 N
ΔF_{pto}	Input increment limit	1000 N

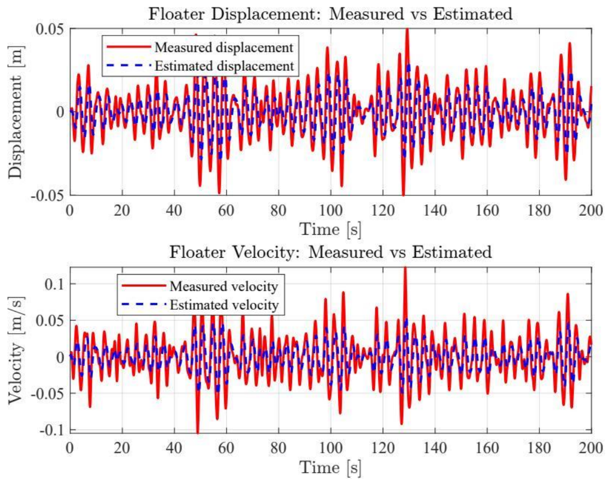

Fig. 4 Velocity and displacement information processed by EKF

Fig. 4 demonstrates the effectiveness of the Extended Kalman Filter in estimating the displacement and velocity of the floater system. The estimated results closely match the measured data in both overall trends and transient behavior.

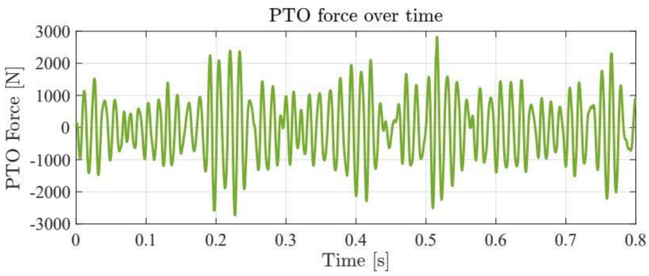

Fig. 5 Control the input force of WEC under LR-EKF based MPC.

Fig. 5 shows the control force input under the LR-MPC framework. The control signal remains smooth over time and strictly satisfies all predefined constraints.

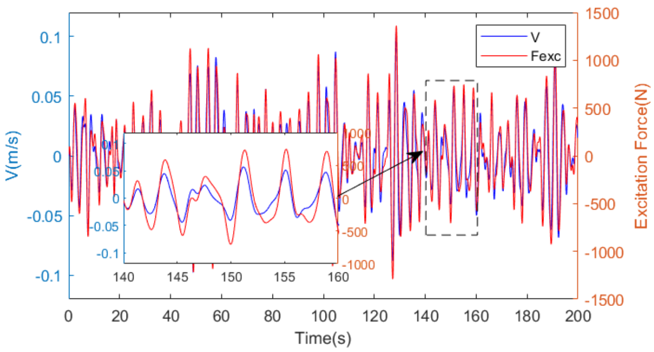

Fig. 6 Phase relationship between estimated excitation force and heave velocity

Fig 6 demonstrates the simulation results of the wave excitation force compared with the float velocity. It is analyzed that the velocity profile and the excitation force are basically the same in phase, indicating that the wave energy conversion system is in a resonant state. Under this condition, the system reaches the maximum energy capture efficiency, and the velocity versus time curve remains smooth without significant fluctuations.

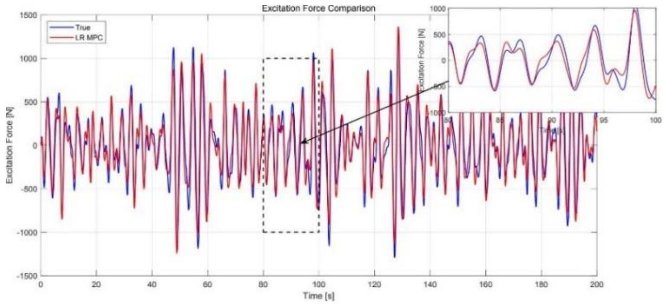

Fig. 7 Predicted vs measured excitation force under linear regression modeling

Fig 7 illustrates that the comparison between predicted and actual incentives indicates that the predicted incentives are aligned in phase with the actual ones.

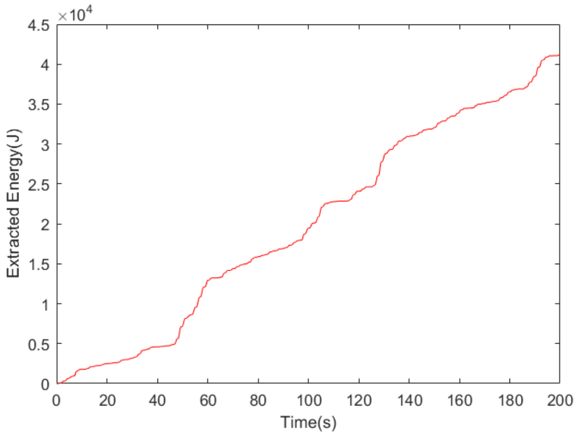

Fig. 8 Energy extracted by the WEC system using the linear regression-based MPC method

Fig. 8 shows the energy extracted by the WEC system under the linear regression-based MPC method, demonstrating that stable and continuous energy extraction is achieved using this control strategy.

In model performance assessment, the coefficient of determination, GOF, as a key quantitative metric, is defined by the mathematical relationship between the total sum of squared deviations (TSS) and the residual sum of squares (RSS), which effectively characterizes the extent to which the predicted data explains the true observations and is often used as a core criterion for validating the accuracy of a kinetic model:

$$GOF = 1 - \frac{RSS}{TSS} = 1 - \frac{\sum_{i=1}^{n}(y_i - \hat{y}_i)^2}{\sum_{i=1}^{n}(y_i - \bar{y})^2} \tag{28}$$

where y is the measured value of excitation force, $\bar{y}$ is the sample mean, and $\hat{y}$ is the model estimate. According to the theoretical definition, the GOF indicator is defined in the [0,1] closed interval, and its value tends to 1 when it reflects a better fit of the model to the data. In particular, when GOF=1, the model predicted value $\hat{y}$ presents a perfect match with the measured value y.

Table 2. Summary of Results During 200s Simulation

Parameters	GOF	Average computing time (s)	Maximum computing time (s)
Value	0.8701	0.0017	0.0057

Table 2 shows the statistics of WEC control results using the linear regression MPC method within a simulation period of 200s. GOF=0.8701 proves that the proposed method based on linear regression MPC has high accuracy in fitting and predicting the exciting force during the control process, and the solution time in the control process proves that using this method can be calculated within the sampling period out control input.

4 Conclusion

In this study, we propose a model predictive control method based on linear regression with extended Kalman filtering, which replaces the excitation force measurements required for the control of traditional wave energy devices by obtaining the transverse rocking angular velocity of the floating body in real time. Simulation results show that this method achieves comparable control accuracy to conventional strategies while reducing hardware cost. By using conventional motion sensors instead of specialized excitation force measurement devices, it not only significantly improves the operational reliability of the system under complex sea conditions, but also drastically reduces the deployment and maintenance cost of the ocean energy equipment. This solution has both control performance and economic advantages, providing a feasible path for the engineering application of wave energy conversion technology.

5 References

[1] H. Tiismus, V. Maask, V. Astapov, T. Korõtko, and A. Rosin, “State-of-the-art review of emerging trends in renewable energy generation technologies,” *IEEE Access*, vol. 13, pp. 10820–10843, 2025, doi: 10.1109/ACCESS.2025.3528640.

[2] A. M. Jariwala, S. K. Dash, U. K. Sahu, and H. M. Mohan, “Performance optimization techniques on point absorber and oscillating water column wave energy converter: A comprehensive review,” *IEEE Access*, vol. 13, pp. 14743–14759, Jan. 2025, doi: 10.1109/ACCESS.2025.3531298.

[3] I. Temiz, J. Leijon, B. Ekergård and C. Boström, “Economic aspects of latching control for a wave energy converter with a direct drive linear generator power take-off,” Renew. Energy, vol. 128, pp. 57–67, December 2018.

[4] X. Huang, K. Sun and X. Xiao, “A Neural Network-Based Power Control Method for Direct-Drive Wave Energy Converters in Irregular Waves,” IEEE Trans. Sustain. Energy, vol. 11, no. 4, pp. 2962–2971, October 2020.

[5] Z. Lin, X. Huang and X. Xiao, “Fast Model Predictive Control System for Wave Energy Converters With Wave Tank Tests”, IEEE Trans. Ind. Electron, vol. 70, no. 7, pp. 6887–6897, July 2023.

[6] Z. Lin, X. Huang, and X. Xiao, “A novel model predictive control formulation for wave energy converters based on the reactive rollout method,” *IEEE Transactions on Sustainable Energy*, vol. 13, no. 1, pp. 491–500, Jan. 2022, doi: 10.1109/TSTE.2021.3117787.

[7] M. Zhang, Z. M. Yuan, S. S. Dai and A. Incecik, “Development of a Novel Wave-force Prediction Model based on Deep Machine Learning Algorithms,” The 30th International Ocean and Polar Engineering Conference, OnePetro, October 2020.

[8] A. F. Davis and B. C. Fabien, “Wave Excitation Force Prediction of a Heaving Wave Energy Converter,” IEEE J. Ocean. Eng, vol. 46, no. 2, pp. 564–572, April 2021.

[9] S. Zhan, G. Li and C. Bailey, “Economic feedback model predictive control of wave energy converters,” IEEE Trans. Ind. Electron., vol. 67, no. 5, pp. 3932–3943, May 2020.

[10] Hasselmann K, Barnett T, Bouws E, et al. Measurements of wind-wave growth and swell decay during the Joint North Sea Wave Project (JONSWAP)[J]. Deut. Hydrogr. Z, 1973, 8: 1–95.